

SPE 29488

Solid Particle Deposition During Turbulent Flow Production Operations

Joel Escobedo and G. A. Mansoori, U. of Illinois at Chicago

SPE Members

Copyright 1995, Society of Petroleum Engineers, Inc.

This paper was prepared for presentation at the Production Operations Symposium held in Oklahoma City, OK, U.S.A., 2-4 April 1995.

This paper was selected for presentation by an SPE Program Committee following review of information contained in an abstract submitted by the author(s). Contents of the paper, as presented, have not been reviewed by the Society of Petroleum Engineers and are subject to correction by the author(s). The material, as presented, does not necessarily reflect any position of the Society of Petroleum Engineers, its officers, or members. Papers presented at SPE meetings are subject to publication review by Editorial Committees of the Society of Petroleum Engineers. Permission to copy is restricted to an abstract of not more than 300 words. Illustrations may not be copied. The abstract should contain conspicuous acknowledgment of where and by whom the paper is presented. Write Librarian, SPE, P.O. Box 833836, Richardson, TX 75083-3836, U.S.A. Telex, 163245 SPEUT.

ABSTRACT

The production and transportation of petroleum fluids could be severely affected by deposition of suspended particles (i.e. asphaltene, paraffin/wax, sand, and/or diamondoid) in the production wells and/or transfer pipelines. In many instances the amount of precipitation is rather large causing complete plugging of these conduits. Therefore, it is important to understand the behavior of suspended particles during flow conditions.

In this paper we present an analysis of the diffusional effects on the rate of solid particle deposition during turbulent flow conditions (crude oil production generally falls within this regime). The turbulent boundary layer theory and the concepts of mass transfer have been utilized to calculate the particle deposition rates on the walls of the flowing conduit. The developed model accounts for the eddy and Brownian diffusivities as well as for inertial effects.

The analysis presented in this paper shows that rates of solid-particle deposition (during crude oil production) on the walls of the flowing channel due solely to diffusional effects are small.

It is also shown that deposition rates decrease with increasing particle size. However, when the process is momentum controlled (large particle sizes) higher deposition rates are expected.

INTRODUCTION

Numerous experimental works have revealed the colloidal nature of the heavy asphaltene fraction of a crude oil. We consider the asphaltenes to exist in crude oil as both dissolved and suspended particles (1, 2, 3). Dispersed asphaltenes are sterically stabilized by neutral resins, they are electrically charged (4), and have a diameter of 30-40 Å (5). The stability of these particles can be disrupted by addition of solvents (i.e. n-heptane), it could also be disrupted during flow conditions due to shear stresses, or by counterbalancing the weak asphaltene particle charge. The latter is an important phenomenon since during crude oil production a streaming potential is generated which is believed to cause asphaltene aggregation (6). When solvents are used to precipitate asphaltenes, the resulting aggregates may have a diameter as large as 300 μ (7). In addition to asphaltenes there may be other types of particles suspended in the crude oil as well. For instance, sand particles swept from the reservoir matrix, paraffin crystals if the temperature falls below the cloud point of the crude, and/or diamondoids.

Production and transportation of petroleum fluids could be severely affected by deposition of asphaltene (and other suspended particles). In many instances the amount of precipitation is rather large causing complete plugging of the flowing channel. Therefore, it is important to understand the behavior of the suspended particles (asphaltenes, sand, paraffin/wax, diamondoid etc.) during flow conditions.

This paper presents a theoretical analysis of the diffusional

References and Illustrations at end of paper

effects on the particle deposition with the utilization of the concepts of mass transfer and the boundary layer theory. The model presented here is intended to explain the solid particle deposition on the walls of the well tubing (or pipeline). It accounts for the Brownian and turbulent diffusion, and for inertial effects.

THEORETICAL ANALYSIS

Substantial work has been done on the area of particle deposition on the walls of channels or pipes in turbulent flow by many researchers (8-15).

A key assumption in the development of the present model is that a fully developed turbulent flow of crude oil has a structure as proposed by Lin *et al.* (8). From experimental observations, they proposed a generalized velocity distribution for turbulent flow of fluids in pipes, as depicted in Figure 1 of their paper. This velocity distribution is comprised of three main regions [Details of this generalization are given elsewhere, (8)]: a) A sublaminal layer adjacent to the wall, b) The transition or buffer region, and c) the turbulent core.

In the sublaminal layer, in which there is no turbulence or eddy diffusion, particle flux is due to Brownian diffusion. Velocity distribution and mass transfer in the turbulent core are governed primarily by eddy diffusivities both of momentum and mass. Whereas in the buffer region the mass transfer is governed by a combined action of Brownian and eddy diffusivities.

It has been observed experimentally that even in the sublaminal layer near the wall a slight amount of eddies is present (8). However, it cannot be measured or correlated based on experimental observations. Nevertheless, empirical correlations have been proposed for the eddy diffusivity in the turbulent boundary layer as we will see later. These correlations are based on analogies with the laminar diffusion boundary layer (8,15).

The theoretical analysis that follows has been done for a system of constant density, and viscosity. Therefore it is applicable to the region above the bubble pressure where only the liquid phase is present. However, it could be extended to the region below the bubble point (gas-liquid) if reliable correlations for viscosity and density versus pressure and composition are available. Because of the scarcity of such correlations, and because multi-phenomena occur in the two phase region of the well tubing (i.e. release of the light ends of the crude, chemical composition variation, etc) which affect the diffusivity of the suspended particles, no attempt is made to extend this model to that region. The assumption of constant viscosity, and constant density is partly justified since density changes are not appreciable until the bubble point pressure is reached inside the well. It is also assumed that suspended particles are all of the same diameter, and that interactions between them are only due to their Brownian and eddy motion (i.e. we have neglected particle-particle interactions).

If we assume that the thickness of the boundary layer is very small compared to the radius of the pipe, then we can neglect any curvature effects.

Thus, the equation used to describe the particle flux, N , in terms

of the diffusivities and the concentration gradient is:

$$N = (D_B + \epsilon) \frac{dC}{dr} \quad (1)$$

D_B is the Brownian diffusivity ($D_B = \frac{K_B T}{3\pi d \mu}$); K_B is the Boltzmann constant (1.38×10^{-16} g-cm²/molecule-°K-s)
 T is the absolute temperature; d is the particle diameter;
 μ is the viscosity of the suspending medium.
 ϵ is the eddy diffusivity
 C is the particles concentration
 r is the radial distance.

Equation 1 is subject to the boundary condition, at $r = S$, $C = C_s$. C_s is the particle concentration at $r = S$, where S is the particle stopping distance measured from the wall.

The concept of a stopping distance was first postulated by Friedlander and Johnstone in 1957 (10). They argued that a particle needs to diffuse only within one stopping distance from the wall, and from this point on, due to the particle momentum, it would coast to the wall. For small particles the stopping distance is small compared to the boundary layer and consequently diffusion dominates. The proposed expression for the particle stopping distance is (10,11):

$$S = \frac{0.05 \rho_p d^2 V_{avg} \sqrt{f/2}}{\mu} + \frac{d}{2} \quad (2)$$

ρ_p density of particles
 V_{avg} Crude oil average velocity
 f friction factor

Equation 1 may be integrated following the procedure for the calculation of temperature drop across a composite wall. We will find the concentration profiles from point to point across the boundary layer. That is, we will calculate the concentration differences through the sublaminal layer, the buffer region and the turbulent core. By adding these concentration differences we can find the overall particle flux in terms of the average and wall concentrations.

Before we integrate equation 1, we need expressions for N and ϵ as functions of the radial distance (r). Johansen, S.T. (15) proposed the following correlation to express the eddy diffusivity as a function of radial distance (r) for the sublaminal layer:

$$\epsilon = v \left(\frac{r^+}{11.15} \right)^3 \quad r^+ \leq 5 \quad (3)$$

v Kinematic viscosity of the fluid (crude oil)
 r^+ Dimensionless radial distance $r^+ = (r V_{avg} \sqrt{f/2}) / v$

Note that Equation 3 is only valid for dimensionless radial distances smaller than 5, which is the limit of the sublaminal layer.

The molar Flux, N , is taken to vary linearly from the wall to the center line of the channel, as proposed by Beal (13):

$$N = N_0 \left(1 - \frac{2r^+}{D_0^*}\right) \quad (4)$$

N_0 particle flux at the wall

D_0^* dimensionless well diameter $D_0^* = (D_0 V_{avg} \sqrt{f/2}) / \nu$,
 D_0 is the diameter of the well tubing

In order to utilize the above two expressions in the integration of Equation 1 we must define another dimensionless variable, $s^+ = (s V_{avg} \sqrt{f/2}) / \nu$, called the dimensionless stopping distance.

Introducing all the new dimensionless variables and the expressions for N and ϵ into Equation 1, we get:

$$N = N_0 \left(1 - \frac{2r^+}{D_0^*}\right) = \left[\frac{D_B}{\nu} + \left(\frac{r^+}{11.15}\right)^3\right] V_{avg} \sqrt{f/2} \frac{dC}{dr^+} \quad (5)$$

subject to the boundary conditions:

$$\begin{aligned} \text{at } r^+ = s^+ & \quad C = C_s \\ \text{at } r^+ = 5 & \quad C = C_5 \end{aligned}$$

Rearranging Equation 5, integrating and applying the above boundary conditions we find:

$$C_5 - C_s = \frac{N_0}{V_{avg} \sqrt{f/2}} \left[\frac{11.15 S_c^{1/3}}{3} F_1(s^+, S_c) + \frac{2(11.15)^2 S_c^{1/3}}{3 D_0^*} F_2(s^+, S_c) \right] \quad (6)$$

$S_c = \frac{\nu}{D_B}$ is the Schmidt number.

$$F_1(s^+, S_c) = \ln \left[\frac{\left(1 + \frac{5}{11.15} S_c^{1/3}\right)^3 \left(1 + \left(\frac{s^+}{11.15}\right)^3 S_c\right)}{\left(1 + \frac{s^+}{11.15} S_c^{1/3}\right)^3 \left(1 + \left(\frac{5}{11.15}\right)^3 S_c\right)} \right]^{1/2} + \sqrt{3} \tan^{-1} \left(\frac{10 S_c^{1/3} - 1}{\sqrt{3}} \right) - \sqrt{3} \tan^{-1} \left(\frac{2s^+ S_c^{1/3} - 1}{\sqrt{3}} \right) \quad (7)$$

$$F_2(s^+, S_c) = \ln \left[\frac{\left(1 + \frac{5}{11.15} S_c^{1/3}\right)^3 \left(1 + \left(\frac{s^+}{11.15}\right)^3 S_c\right)}{\left(1 + \frac{s^+}{11.15} S_c^{1/3}\right)^3 \left(1 + \left(\frac{5}{11.15}\right)^3 S_c\right)} \right]^{1/2} - \sqrt{3} \tan^{-1} \left(\frac{10 S_c^{1/3} - 1}{\sqrt{3}} \right) + \sqrt{3} \tan^{-1} \left(\frac{2s^+ S_c^{1/3} - 1}{\sqrt{3}} \right) \quad (8)$$

Equations 6-8 describe the transport of suspended particles to the wall in terms of the concentration difference between the limits $r^+ = s^+$ (dimensionless stopping distance) and $r^+ = 5$ (limit of the sublaminal layer)

The next step is the calculation of the particle flux between the

concentration at $r^+ = 5$ and $r^+ = 30$ (limit of the buffer layer). The eddy diffusivity expression for the buffer layer was assumed to be:

$$\epsilon = \left[\left(\frac{r^+}{11.4}\right)^2 - 0.1923 \right] \nu \quad 5 \leq r^+ \leq 30 \quad (9)$$

Integration of Equation 1, using Equation 9 for ϵ gives:

$$C_30 - C_5 = \frac{N_0}{V_{avg} \sqrt{f/2}} \left[11.4 \left(\frac{S_c}{1 - 0.1923 S_c}\right)^{1/2} P_3(s^+, S_c) - \frac{(11.4)^2}{D_0^*} \ln \left(\frac{1 - 0.1923 S_c + \left(\frac{30}{11.4}\right)^2 S_c}{1 - 0.1923 S_c + \left(\frac{5}{11.4}\right)^2 S_c} \right) \right] \quad (10)$$

$$P_3(s^+, S_c) = \tan^{-1} \left(\frac{30}{11.4} \left(\frac{S_c}{1 - 0.1923 S_c}\right)^{1/2} \right) - \tan^{-1} \left(\frac{5}{11.4} \left(\frac{S_c}{1 - 0.1923 S_c}\right)^{1/2} \right) \quad (11)$$

Equations 10 and 11 describe the particle transport in terms of the concentration difference between the limits of the buffer layer.

The following step is the calculation of the particle transport rate in terms of the difference between the concentration at $r^+ = 30$ (upper limit of the buffer layer) and the bulk concentration (average conc.). The eddy diffusivity for the turbulent core is taken to be (15):

$$\epsilon = (0.4 r^+) \nu \quad r^+ \geq 30 \quad (12)$$

If we assume that at $V = V_{avg}$, $C = C_{avg}$, then we could integrate Equation 1 using Equation 12 to obtain:

$$C_{avg} - C_{30} = \frac{N_0}{V_{avg} \sqrt{f/2}} \left[\left(25 + \frac{125}{D_0^* S_c}\right) \ln \left(\frac{1 + 2.5 r_{avg}^+ S_c}{1 + 75 S_c} \right) - \frac{5 r_{avg}^+}{D_0^*} + \frac{150}{D_0^*} \right] \quad (13)$$

r_{avg}^+ is the dimensionless radial distance (measured from the wall) where $V = V_{avg}$. Equation 13 describes the particle transport in terms of the concentration difference between the bulk (average) and the upper limit of the buffer layer.

So far, we have expressions for the three different regions (wall layer, buffer layer, and turbulent core). Now they may be added together to obtain an expression for N_0 in terms of C_{avg} , C_{s^+} , average fluid velocity, s^+ , and physical parameters of the system.

Until now, only dimensionless stopping distances (s^+) less than 5 have been considered. However, for particles large enough, s^+ could be greater than 5. If so, then the preceding analysis is not valid under these conditions. This difficulty may be overcome if Equation 1 is integrated between the limits $C = C_{s^+}$ at $r^+ = s^+$ and $C = C_{30}$ at $r^+ = 30$ using the eddy diffusivity correlation for the buffer layer (equation 9).

Introducing Equation 9 into Equation 1 and integrating using

the assumptions noted previously, we get:

$$C_{30} - C_5^+ = \frac{N_0}{V_{avg} \sqrt{\ell/2}} \left[11.4 \left| \frac{Sc}{1 - 0.1923 Sc} \right|^{1/2} [F_3(s^+, Sc)] \cdot \frac{(11.4)^2}{D_0^2} \ln \left(\frac{1 - 0.1923 Sc + \left(\frac{30}{11.4}\right)^2 Sc}{1 - 0.1923 Sc + \left(\frac{s^+}{11.4}\right)^2 Sc} \right) \right] \quad (14)$$

$$F_3(s^+, Sc) = \tan^{-1} \left(\frac{30}{11.4} \left| \frac{Sc}{1 - 0.1923 Sc} \right|^{1/2} \right) \cdot \tan^{-1} \left(\frac{s^+}{11.4} \left| \frac{Sc}{1 - 0.1923 Sc} \right|^{1/2} \right) \quad (15)$$

If $s^+ = 5$ then Equations 14 and 15 reduce to equation 10 and 11. Equation 13 still applies to the turbulent core.

For particles with a dimensionless stopping distance: $0 \leq S^+ < 5$

We add equations 6, 10, and 13, to obtain an expression for the mass transfer coefficient defined as $N_0 / (C_{avg} - C_5^+) = K$. K is the transfer (transport) coefficient and has dimensions of velocity (cm/sec). The expression for the transport coefficient obtained is:

$$K = V_{avg} \sqrt{\ell/2} \left[\frac{11.15 Sc^{1/3} F_1(s^+, Sc) + \frac{2(11.15)^2 Sc^{1/3} F_2(s^+, Sc) + 11.4 \left| \frac{Sc}{1 - 0.1923 Sc} \right|^{1/2} [F_3(s^+, Sc)]^{-1}}{3 D_0^2} \cdot \frac{(11.4)^2}{D_0^2} \ln \left(\frac{1 + 6.7329 Sc}{1 + 0.000067 Sc} \right) + \left(2.5 + \frac{12.5}{D_0^2 Sc} \right) \ln \left(\frac{1 + 2.5 r_{avg} Sc}{1 + 75 Sc} \right) \cdot \frac{5 r_{avg} + 150}{D_0^2} \right] \quad (16)$$

F_1 , F_2 , and F_3 are the same as defined previously.

For particles with a dimensionless stopping distance: $5 \leq S^+ < 10$

We add Equations 14 and 13, solving for K we get:

$$K = \frac{V_{avg} \sqrt{\ell/2}}{\left[11.4 \left| \frac{Sc}{1 - 0.1923 Sc} \right|^{1/2} [F_3(s^+, Sc)] \cdot \frac{(11.4)^2}{D_0^2} \ln \left(\frac{1 - 0.1923 Sc + \left(\frac{30}{11.4}\right)^2 Sc}{1 - 0.1923 Sc + \left(\frac{s^+}{11.4}\right)^2 Sc} \right) + \left(2.5 + \frac{12.5}{D_0^2 Sc} \right) \ln \left(\frac{1 + 2.5 r_{avg} Sc}{1 + 75 Sc} \right) \cdot \frac{5 r_{avg} + 150}{D_0^2} \right]} \quad (17)$$

F_3 is the same as previously defined

With the previous analysis we have found analytical expressions for the mass transfer coefficient for different particle sizes in terms of the dimensionless stopping distance.

Next we must account for inertial effects. Beal (13), proposed the following expression to account for inertial effects [details

given elsewhere (13)]:

$$K_D = \frac{N_0}{C_{avg}} = \frac{K p \vartheta}{K + p \vartheta} \quad (18)$$

K_D was defined by Beal as the deposition coefficient (mass transfer coefficient which contains the inertial effects, N_0 is as previously defined)

p is the asphaltene-particle sticking factor (taken as 1)

ϑ is the average velocity of the particles near the walls, and consists of two parts:

$\vartheta = \vartheta_f + \vartheta_B$; ϑ_f is the component due to fluid motion and ϑ_B is the component due to particle Brownian motion.

$$\vartheta_B = \left(\frac{K_B T}{2\pi m} \right)^{1/2} ; \quad \vartheta_f = \frac{V_{avg} \sqrt{\ell/2}}{4} [\vartheta_f^+(d^+/2) + \vartheta_f^+(S^+)]$$

where m is the particle mass, $\vartheta_f^+(d^+/2)$ is the particle velocity at a dimensionless radial distance $d^+/2$; d^+ is the dimensionless particle diameter; $\vartheta_f^+(S^+)$ is the particle velocity at a dimensionless radial distance S^+ (dimensionless stopping distance). The quantity ϑ_f^+ can be calculated using expressions proposed by Laufer, (1954):

$$\vartheta_f^+ = 0.05 r^+ \text{ for } 0 \leq r^+ \leq 10$$

$$\vartheta_f^+ = 0.5 + 0.0125 (r^+ - 10) \text{ for } 10 \leq r^+ < 30$$

The particles can be anywhere between $r^+ = d^+/2$ and $r^+ = s^+$ considering this we may use either expression for ϑ_f^+ .

The analysis for particle deposition onto the walls of a flowing channel from turbulent fluid streams is concluded by taking into account the inertial effects as in Equation 18. At this point all the parameters influencing the deposition rate (Brownian diffusivity, eddy diffusivity, and inertial effects) have been taken into account.

COMPARISON OF THE PROPOSED MODEL WITH EXPERIMENTAL DATA AND OTHER MODELS

In order to apply the preceding analysis to particle deposition during turbulent flow production operations we must compare the theoretical predictions against some experimental data. Unfortunately experimental data for particle deposition from turbulent flows is very scarce. There is however more data for deposition from aerosols than from liquid suspensions. We do comparisons here for particle deposition from turbulent gas streams.

The results of this analysis for particle deposition from turbulent fluid streams are in good agreement with the experimental deposition rates for iron particles in air (10,11). The predictions

of the present model show a better agreement with the mentioned experimental data than the models proposed by Friedlander and Johnstone (10), and Beal (13).

Figure 1 shows a comparison of the proposed model predictions with the experimental data and model proposed by Friedlander and Johnstone (10) for 0.8μ iron particles suspended in a turbulent air stream at 298°K (pipe diameter is 0.54 cm). It can be seen the fairly good agreement of the predicted deposition rates with experimental data. It is also noticeable the better prediction capabilities of the present model compared to those of Friedlander and Johnstone (10). In Friedlander and Johnstone model, Brownian diffusion is not taken into account; it only takes into consideration the particle momentum and eddy diffusion as the governing mechanisms for particle mobility. The reasons for the good predictions of the present model are attributed to the fact that it takes into account Brownian diffusion as well as the other two parameters (particle momentum and eddy diffusivity). The particles studied by Friedlander and Johnstone (0.8μ) are small enough to be affected by Brownian diffusion, therefore, it cannot be neglected.

Figure 2 shows a comparison of the present model predictions with the experimental data of Friedlander and Johnstone for iron particles in air (10,11), and with the model proposed by Beal (13). Although, Beal's model also takes into account Brownian diffusivity, however, it utilizes a different expressions for the eddy diffusivities in the sublaminal layer and in the buffer region. It also uses a different expression for the turbulent core. It can be seen from this figure that the proposed model posses better prediction capabilities.

Figure 3 shows the experimental deposition coefficient data (10,11) for 0.8μ and 1.57μ iron particles suspended in a turbulent air stream at 298°K (pipe diameter is 1.3 cm). It also shows the experimental data for 1.81μ aluminum particles suspended in a turbulent air stream at 298°K (pipe diameter is 1.38 cm). From Figure 3 one can notice the fairly good prediction capabilities of the proposed model for all the three sets of data.

In Figure 4 we examine the effect of pipe diameter on the transport coefficient. The results presented in this figure correspond to 0.8μ iron particles suspended in flowing air at 298°K . As we can see from Figure 4 there is a dramatic decrease in the transport coefficient as the diameter of the pipe increases. This is not surprising, since the larger the diameter the longer the distance particles have to travel prior to deposition.

We have also studied the effect of particle diameter on the transport coefficient for various Reynolds numbers as reported in Figure 5. These results were obtained for iron particles in air at 298°K flowing through a pipe of 0.54 cm inner diameter. From this figure we can notice that the curves have the same shape as those predicted by Beal (13) for Aitken nuclei, drops of tricresyl phosphate, and polystyrene spheres. There is no numerical data for these particles reported in Beal's paper and no experimental data for iron particles. As a result we may conclude that this analysis for the effect of particle diameter is qualitatively correct. From Figure 5 we can notice a decrease in transport coefficient with increasing particle diameter and at a certain particle diameter a minimum is reached after which a sharp increase in the transport coefficient is observed. An explanation for this is that in the left-hand-side of

the minima (small particles) the process is diffusion controlled whereas in the right-hand-side of the minima (large particles) the process is momentum controlled.

MODEL PREDICTIONS FOR SOLID PARTICLE DEPOSITION INSIDE TUBINGS AND WELLS

Despite the good agreement of the present model predictions with experimental data of Friedlander and Johnstone (10,11), it does not indicate that it could be applicable to predict the behavior of solid particles in turbulent flow production operations. In order to justify the validity of the proposed model for this purpose one has to determine experimentally the solid particle deposition coefficients in a turbulent crude oil flow, and compare them with the model predictions. However, no experimental data is reported in the literature regarding this subject. Therefore, we believe the model is good enough to make, at least, qualitative predictions of the solid-particle deposition coefficient from turbulent crude oil flow, and is used as such.

Figure 6 shows the predicted transport coefficients for solid particles as a function of particle diameter for various crude oil production rates. The particle sizes analysed ranged from 50\AA to 200μ . The results presented in this figure were obtained for a crude oil with a gravity of 30.21°API and with a kinematic viscosity of 11 centi Stokes. We can notice from Figure 6 that the transport coefficients are in general small except at high production rates and for very large particles. As in Figure 5 we notice a minimum after which the transport coefficient increases more rapidly with increasing particle diameter this is due to the fact that at this point the deposition process is momentum controlled. Judging from Figure 6, the amounts of particle deposition expected from turbulent crude oil production may be very small when the diameter of the suspended particles is less than 1μ . However, higher amounts of deposition may be expected when the suspended particles have diameter larger than 1μ specially at high production rates when the turbulence is very high.

We performed model predictions varying the kinematic viscosity of the crude oil to study the effect of this parameter on the deposition coefficient. Figure 7 shows the predicted values for a crude oil containing suspended particles of 1μ in diameter. We can see a decrease in the deposition coefficients with increasing kinematic viscosity. This means that the lighter the crude oil the higher the probability of having particle deposition. We also notice an increase in the transport coefficient with increasing production rate. However, these predicted values are still very small.

CONCLUSIONS

The model developed for particle deposition onto the walls of a pipe from a turbulent fluid stream shows a fairly good agreement with the available experimental data. Furthermore, the agreement with the experimental data is better than the models proposed earlier by Friedlander and Johnstone, and by Beal. For these

reasons, it can be used to predict solid particle deposition rates from turbulent flow production operations, in a qualitative fashion. The effect of particle size on the deposition coefficient was investigated finding that when the deposition process is diffusion controlled (particles with diameter $< 1\mu$) the predicted values are very small. However, when the deposition process is momentum controlled (particles with diameters $> 1\mu$) the predicted values for the transport coefficient increase more rapidly with increasing particle diameter. We also investigated the effect of crude oil kinematic viscosity on the transport coefficient. We found that transport coefficients decrease with increasing crude oil kinematic viscosity. For kinematic viscosities 12.16 cSt the predicted transport coefficients are negligible for suspended particles of 1μ . We also found that transport coefficients increase with increasing production rate this is due to the fact that at larger production the amount of eddy diffusion is bigger. The proposed model can be used for various cases of particle depositions from turbulent flows whether it is asphaltene, paraffin/wax crystal, or sand so long as the particles are neutral and their sizes are stable and there are no phase transitions occurring in the flow. However, in cases where such changes are occurring in the system this model will require substantial modifications.

ACKNOWLEDGMENT: This research is supported in part by Chevron Oil Field Services and in part by the National Science Foundation Grant No. CTS-9108595.

REFERENCES

- Escobedo, J. and Mansoori, G.A. "Heavy Organic Deposition and Plugging of Wells (Analysis of Mexico's Experience)" Proceedings of the II LAPEC, SPE Paper # 23696, Society of Petroleum Engineers, Richardson, TX March, 1992.
- Mansoori, G.A., "The Occurrence of Asphaltene Throughout Production Cycle" Proceedings of the 6th Abu Dhabi International Petroleum Exhibition and Conference, ADSPE # 2, Society of Petroleum Engineers, Richardson, TX October 1994.
- Kawanaka, S., Park, S.J., Mansoori, G.A. "Thermodynamic and Colloidal Models of Asphaltene Flocculation," In Oil Field Chemistry, ACS Symposium Series No. 396, Am. Chem. Soc., Washington, D.C. (1989), Chapter 24.
- Lichaa, P.M. and Herrera, L. "Electrical and Other Effects Related to the Formation and Prevention of Asphaltene Deposition in Venezuela," Paper SPE 5304 presented at the 1975 SPE Intl. Symposium on Oilfield Chemistry, Dallas, TX, Jan. 16-17.
- Ray, R.B., Witherspoon, P.A., and Grim, R.E. "A Study of the Colloidal Characteristic of Petroleum Using the Ultracentrifuge," J. Phys. Chem. (1957) 61, 1296-1302.
- Katz, D.H. and Beu, K.E. "Nature of asphaltic substances," Ind. Eng. Chem., 37: 195-200, 1945.
- Ferworn, K.A., Svrcek, W.Y., and Mehrotra, A.K. "Measurement of Asphaltene Particle Size Distributions in Crude Oils Diluted with n-Heptane," Ind. Eng. Chem. Res. (1993) 32, 955-959.
- Lin, C.S., Moulton, R.W. and Putnam, G.L. "Mass transfer between solid wall and fluid streams," Ind. Eng. Chem., 45, 3, 1953.
- Laufer, J. "The Structure of Turbulence in Fully developed pipe flow," NACA 1174, National Advisory Committee for Aeronautics, 1954. (Available from NASA as TR-1174).
- Friedlander, S.K. and Johnstone, H.F. "Deposition of suspended particles from turbulent gas streams," Ind. Eng. Chem., 49(7): 1153-1156, July 1957.
- Friedlander, S.K. "Deposition of aerosol particles from turbulent gases," Ph.D. Dissertation, U. of Illinois at Urbana-Champaign, 1954.
- Harriott, P. and Hamilton, R.M. "Solid-liquid transfer in turbulent pipe flow," Chem. Eng. Sc., 20:1073-1078, 1965.
- Beal, S.K. "Deposition of particles in turbulent flow on channel or pipe walls," Nuclear Sc. Eng., 40, 1-11, 1970.
- Shapiro, M., Brenner, H. and Guell, D.C. "Accumulation and Transport of Brownian Particles at Solid Surfaces: Aerosol and Hydrosol Deposition Processes," J. Colloid Inter. Sci. 136(2): 552, 1990.
- Johansen, S.T. "The Deposition of Particles on Vertical Walls," Int. J. Multiphase flow 17(3): 355, 1991.

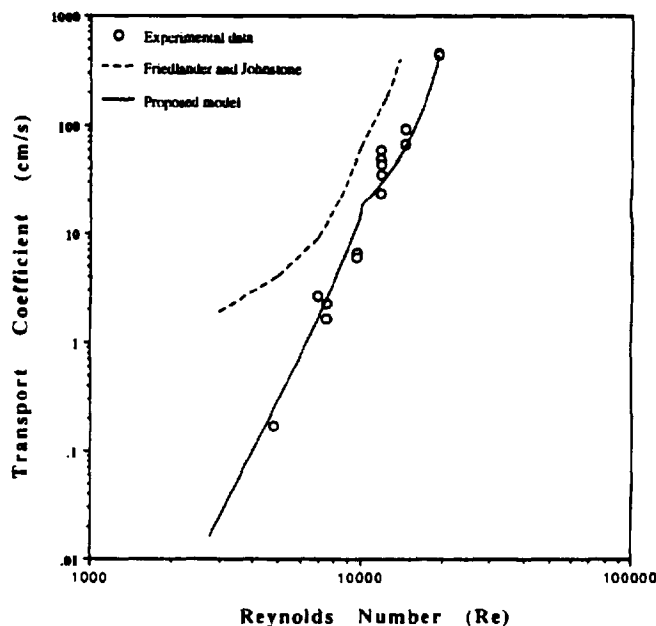


Figure 1. Comparison of the proposed model with the experimental data and model proposed by Friedlander and Johnstone (10) for 0.8μ iron particles suspended in a turbulent air stream at 298°K .

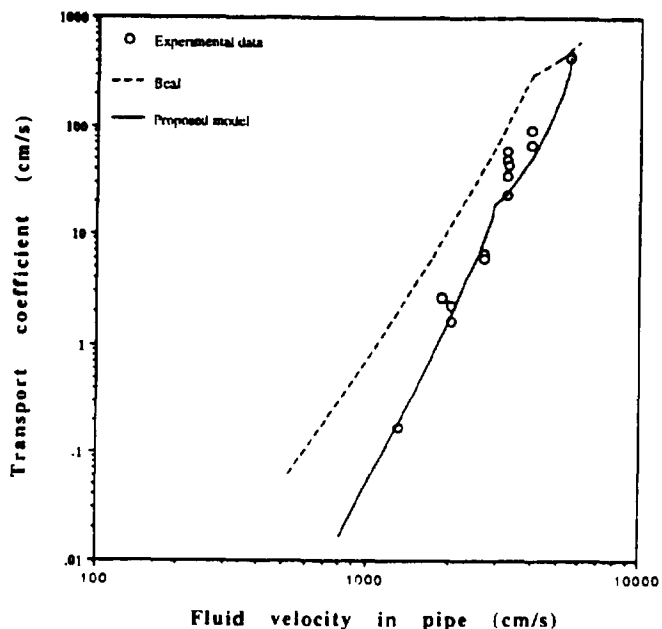


Figure 2. Comparison of the proposed model with the experimental data and model proposed by Beal (13) for 0.8 μ iron particles suspended in a turbulent air stream at 298°K (10).

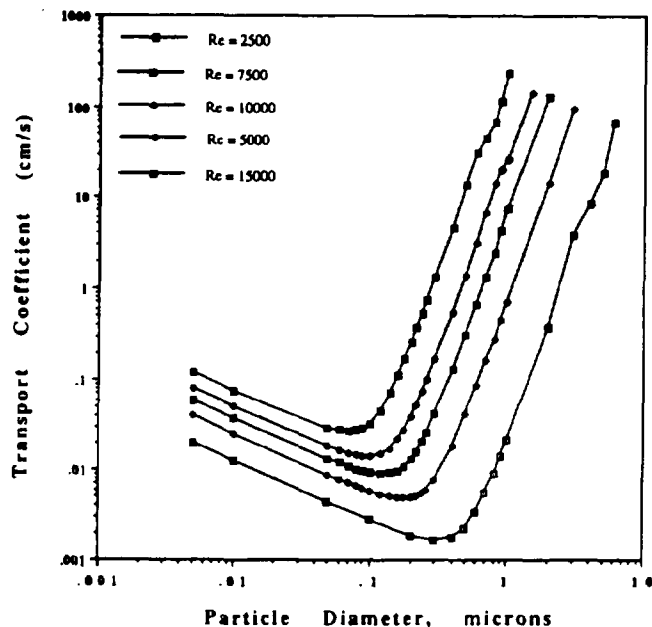


Figure 4. Effect of particle diameter on the transport coefficient for iron particles suspended in turbulent air streams flowing through a pipe with an internal diameter of 0.54 cm.

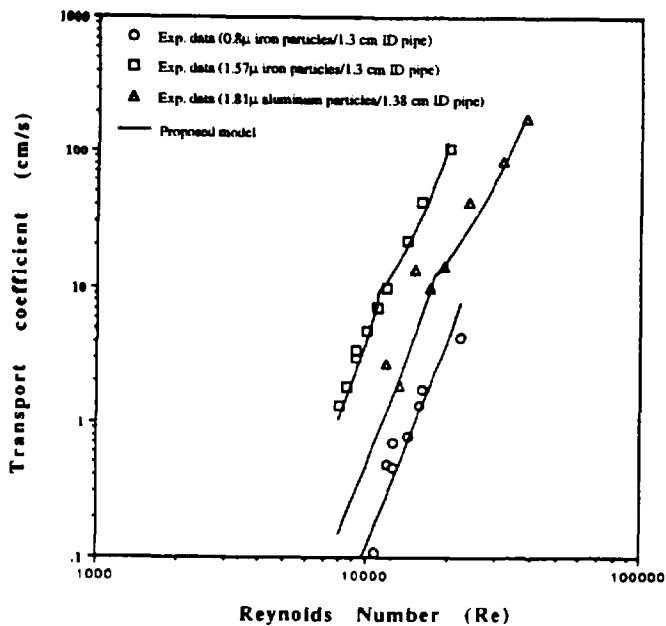


Figure 3. Comparison of the proposed model prediction with Friedlander and Johnstone's data (10) for various particles in air.

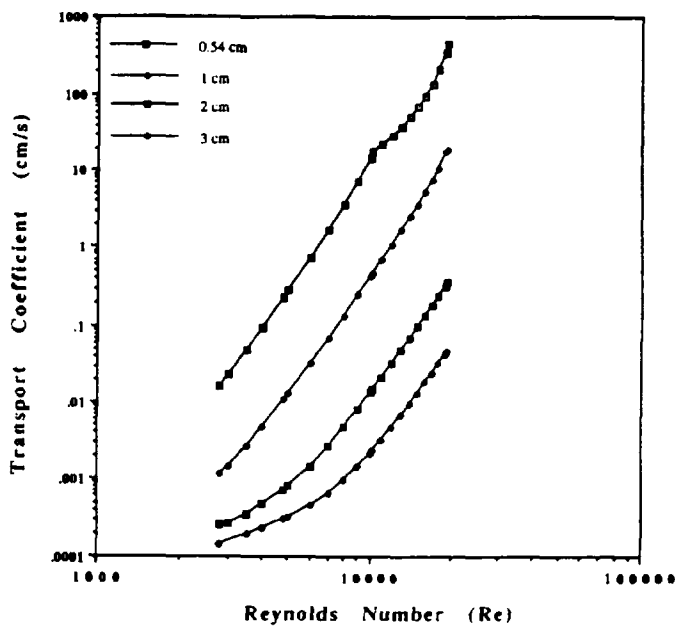


Figure 5. Effect of pipe diameter on the transport coefficient for 0.8 μ iron particle suspended in a turbulent air stream.

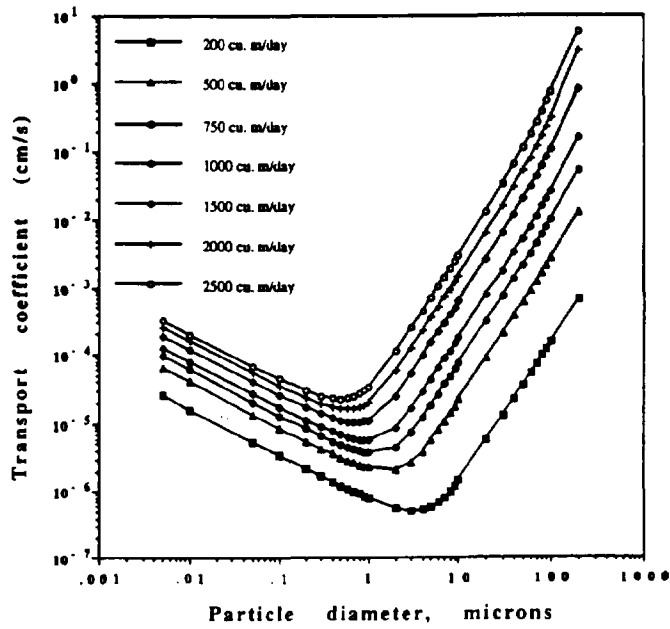


Figure 6. Effect of particle size on the transport coefficient for a 30.21 °API crude oil with a kinematic viscosity of 11 cSt at various production rates.

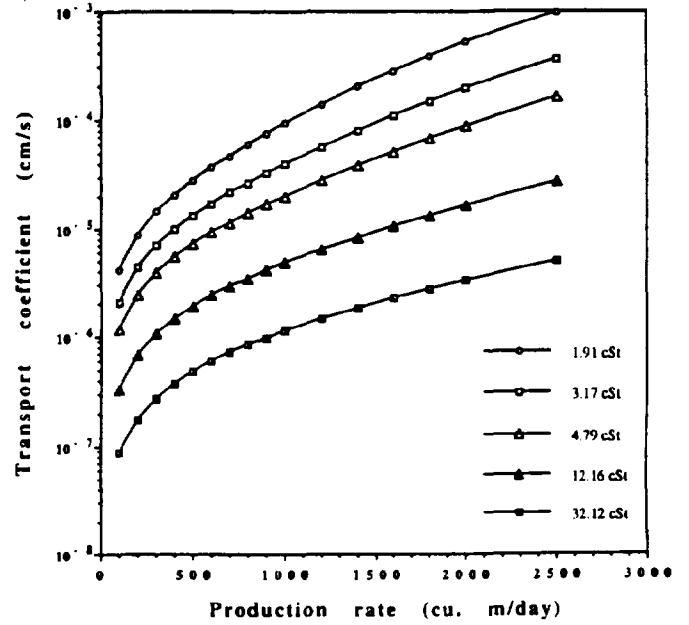


Figure 7. Effect of crude oil kinematic viscosity on the transport coefficient for 1μ suspended particles.